

Received April 8, 2020, accepted April 28, 2020, date of publication May 11, 2020, date of current version May 29, 2020.

Digital Object Identifier 10.1109/ACCESS.2020.2993630

The Leakage Current Components as a Diagnostic Tool to Estimate Contamination Level on High Voltage Insulators

ALI A. SALEM¹, (Member, IEEE), R. ABD-RAHMAN¹, SAMIR AHMED AL-GAILANI², M. S. KAMARUDIN¹, (Member, IEEE), HUSSEIN AHMAD³, AND ZAINAL SALAM³, (Member, IEEE)

¹Department of Power Electrical, Faculty of Electrical and Electronic Engineering, University Tun Hussein Onn Malaysia, Batu Pahat 86400, Malaysia

²School of Electrical and Electronic Engineering, Universiti Sains Malaysia, Penang 14300, Malaysia

³School of Electrical Engineering, Faculty of Engineering, Universiti Teknologi Malaysia, Johor Bahru 81310, Malaysia

Corresponding authors: Ali A. Salem (en.alisalem@gmail.com) and Samir A. Al-Gailani (samer.algailani@usm.my)

This work was supported in part by the University Tun Hussein Onn Malaysia and Ministry of Higher Education Malaysia under Grant U117, and in part by the University of Science Malaysia under Grant 304/PELECT/6315344.

ABSTRACT The current paper presents an alternative and innovative technique to predict the severity of pollution of high voltage insulator using a higher harmonics component with up to the 7th component of leakage current. The leakage current was measured using a current transformer and a shunt resistor. Next, laboratory tests were conducted on glass and porcelain insulators with artificial pollution under salt-fog pollution state which is further represented by three levels, namely light, medium, and high contamination. In this case, the formulation of a new severity of harmonic index refers to a ratio of the sum of 5th and 7th to the 3rd harmonic component. More importantly, the new index managed to provide more accurate results when used as a diagnostic tool for the levels of pollution, compared to the ratio of the total harmonic distortion (THD) to the number of odd harmonics components (n) as the boundaries. In this case, the insulators were found to be in a clean and normal condition when the $K_{(5+7)/3}$ value was greater than 3%. Contrastingly, the insulators were in an extreme condition when the $K_{(5+7)/3}$ was lower than 3%. Nevertheless, there is a high probability of a flashover in glass and porcelain insulators if the $K_{(5+7)/3}$ value is less than 2%. The present study shows the possibility of utilizing the value of strange harmonics up to the 7th component of leakage current as the parameter for the monitoring of leakage current in overhead insulators in the presence of contamination. Overall, it can be concluded that the 3rd, 5th, and 7th harmonics details extracted from the leakage current act as a good indicator for the level of contamination.

INDEX TERMS Polluted insulators, leakage current, harmonic components, total harmonic distortion, fast fourier transform, salt fog.

I. INTRODUCTION

High voltage insulator is one of the vital components in the power system and delivery. Generally, it is utilized to isolate the conductor from the grounded tower as well as provide mechanical support for the power lines. Regarding this matter, it should be noted that the performance of the outdoor insulator is highly influenced by various mechanical and environmental factors such as the type of material, installation arrangement, and pollution severity [1]–[3].

The associate editor coordinating the review of this manuscript and approving it for publication was Pierluigi Siano¹.

Moreover, the polluted environment tends to cause the insulators to be susceptible to the high magnitude of leakage current and lead to an increase of discharge activities over its surface. Accordingly, these conditions may result in an undesirable flashover phenomenon which can cause an interruption in power transmission [4]–[7]. Therefore, the condition monitoring of the leakage current requires considerable attention in ensuring the overall health of the insulator. Accordingly, this will improve the understanding of the power supply reliability.

The deposited surface pollutant such as dust and chemical emission can be regarded as one of the biggest threats to

TABLE 1. Performance comparison of proposed approach to evaluate the contaminated insulators conditions from previous studies with respect to parameter index, define index, application, limitation, efficiency, method and acquisition system.

Ref	Parameter Index	Define index	Application	Limitation	True predict /all tests	Method	Acquisition system
[12]	Frequency harmonics	N/A	String/ Single insulator	N/A	N/A	Analytical	Online/offline
[20]	Phase shift	$\cos(\theta_v - \theta_I)$	Single insulator	N/A	8/11	Determined	Offline
[21]	FOV	Fitting curve	String/Single insulator	Flashover	N/A	Regression	Offline
[27]	THD	THD	Single insulator	N/A	N/A	Analytical	Online/offline
[30]	3rd, 5th	5th /3rd	Composite	N/A	32/41	Determined	Offline

outdoor insulation, thus leading leads to material degradation resulted from surface tracking and erosion. In addition, the insulator surface characteristics may undergo a few changes due to the arcing and corona activities which can lead to premature ageing [8]–[11]. Regarding this matter, it is important to note that all of these factors are a well-known phenomenon that promotes the increase in the magnitude of leakage current (LC) flow over the insulator surface. Accordingly, the assessment of outdoor insulator properties and its long-term performance has been a major area of interest in the scholarly community [12]–[16].

In particular, one issue of interest refers to the establishment of an accurate relationship between the leakage current and pollution severity when the insulator is in service. In this case, several authors [17]–[19] have predicted the pollution severity by employing the statistical values of the LC which include the mean, maximum, and standard deviation (STD) values. Specifically, these values allow the dimensions and severity of the pollution layer to be estimated. In another approach [20], the phase shift between the currents and voltage waveforms was monitored to predict the pollution level. In particular, the result indicates that the variations in the cosine of the phase angle (displacement factor) are a good indicator in determining the pollution and humidity difference with respect to the clean and dry condition [20].

On a similar note, the flashover v measurement method can be utilized to access the pollution severity on outdoor insulator [10], [21], [22]. However, it should be understood that this approach requires the insulator to achieve the range of the flashover voltage. Furthermore, prior knowledge on the parameters such as the dry bands are deemed necessary. Meanwhile, another interesting approach that can be used to predict the pollution severity refers to a technique known as the leakage current extraction which has been widely adopted by several researchers [23]–[25]. In this case, the leakage current time profiles are analyzed in the frequency domain using Fast Fourier Transform (FFT), power spectrum, or wavelet analysis. Overall, it has been concluded based on the frequency content that the presence of leakage currents intensifies the odd harmonic components of the leakage current. The results found that the harmonics of concern are

150 and 250 Hz for the 50 Hz system [25]. Accordingly, this seems to suggest that the intensification leads to the increase of the total harmonic distortion (THD) which tends to vary depending on the pollution level [26].

Table 1 summarizes existing significant work which explored different approaches in monitoring the health of the insulator. Apart from that, it is deemed extremely useful to have an index (a number) that reflects the health condition of the insulators as suggested by [27], [28]. It would be very useful to have an index (a number) that Regarding this matter, authors in [14] adopted the frequency components decomposition concept to compute the related indices. Specifically, the ratio of the 5th/3rd harmonic of the leakage current and the THD was computed in predicting the flashovers occurrences. The reported results on silicon rubber and porcelain insulators indicated a strong relationship between the pollution severity and the value of this ratio. Nevertheless, a search of the literature revealed that the severity research on the porcelain and glass insulators concerning the 7th component of surface leakage current has never been attempted. More importantly, this approach is expected to produce a more accurate prediction compared to the 5th/3rd ratio. Therefore, the current research aims to develop a new indicator based on the odd harmonic ratio up to the 7th considering the significant effect of different wetting levels of pollution on the performance of leakage current. In addition, three different rates of wetting will be applied to establish a reliable result, followed by an observation on the THD of the leakage current concerning the pollution level boundary on 22, 33, and 66 kV insulator strings.

II. LEAKAGE CURRENT HARMONICS

A. BACKGROUND THEORY

In electrical discipline, the term harmonics refers to a sinusoidal waveform which is described as multiple frequencies of the system. For example, the frequency which is three times the fundamental is known as third harmonics, followed by fifth harmonics as the five times the fundamental, and others [29]. Hence, the harmonics (especially the odd harmonics 3rd, 5th, and 7th) are regarded as a dominant factor in the production of distortions on the current and voltage

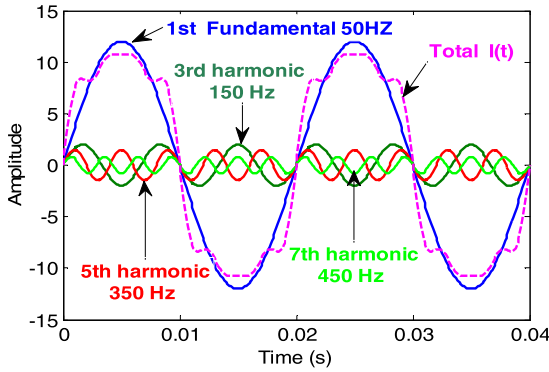


FIGURE 1. Current waveform with harmonics and expansion of the overall current into its harmonic components 1 (fundamental), 3, 5, and 7 [29].

waveforms. Figure 1 shows the leakage current waveform $I(t)$ and its odd harmonics 1st, 3rd, 5th and 7th.

The frequency of the harmonics component is given as follows:

$$f_h = h \times f_F \tag{1}$$

where f_h is the frequency of the harmonic, h represents the harmonics order number, and f_F postulates the fundamental frequency. In Figure 1, the distorted leakage current waveform $I(t)$ can be observed with its constituent harmonics in time and frequency domains. The general expression of leakage current harmonics waveform can be written as shown below:

$$I_h = I_{mh} \sin(2\pi(h \times f_F)t + \phi_h) \quad h = 1, 3, 5, 7, \dots, n \tag{2}$$

Meanwhile, the current for odd components from 1st to 7th can be expressed as:

$$\begin{cases} I_1 = I_{m1} \sin(2\pi(1 \times f_F)t + \phi_1) \text{ For 1}^{st} \text{ component} \\ I_3 = I_{m3} \sin(2\pi(3 \times f_F)t + \phi_3) \text{ For 3}^{rd} \text{ component} \\ I_5 = I_{m5} \sin(2\pi(5 \times f_F)t + \phi_5) \text{ For 5}^{th} \text{ component} \\ I_7 = I_{m7} \sin(2\pi(7 \times f_F)t + \phi_7) \text{ For 7}^{th} \text{ component} \end{cases} \tag{3}$$

The total leakage current can be given as:

$$I(t) = \sum_{h=1}^7 I_h \quad h = 1, 3, 5 \quad \text{and} \quad 7 \tag{4}$$

where I_h , I_{mh} , and ϕ_h respectively represent the current of h^{th} harmonic component, the amplitude of h^{th} harmonic component, and the phase angle between fundamental and h^{th} harmonic component. The fundamental frequency $f_F = 50\text{Hz}$ is in accordance with the Malaysian power system. The total harmonic distortion THD is calculated by [30],

$$THD = \frac{\sqrt{\sum_{h=2}^n (I_h)^2}}{I_1} \tag{5}$$

where n represents the last odd harmonic component number.

B. LEAKAGE CURRENT CRITERIA DIAGNOSTIC

On another note, the present study proposed the criteria for the detection of insulators conditions. More importantly, it should be noted that the indexes took into account the parameters that have a direct impact on leakage current value which include odd harmonics components, total harmonic distortion, and phase shift between leakage current and voltage.

As previously mentioned, the variations of third, fifth, and seventh harmonics components are commonly used as the criterion to evaluate the contamination severity for the service condition of insulators. In addition, the rate of total harmonic distortion THD to the number of odd harmonics ± 1 ($n \pm 1$) plays an important role in the diagnosis of pollution intensity which will be used as the limits for index. Meanwhile, the number of harmonics ± 1 ($n \pm 1$) is used as confidence intervals for medium pollution level, followed by the ($n \pm 1$) which is adopted as inequality among the three pollution levels. For example, light pollution higher than the upper limit at $THD/n-1$, medium pollution between upper limit at $THD/n-1$ and the lower limit at $THD/n+1$, and heavy pollution below the lower limit at $THD/n+1$. Regarding this matter, it is important to understand that the increase in total harmonic distortion and third harmonic component, especially of LC is resulted by surface pollution including other effects such as humidity and temperature. Therefore, the index $K_{(5+7)/3}$ is defined as follows:

$$K_{(5+7)/3} = \frac{(5^{th} + 7^{th}) \text{ harmonics components}}{3^{rd} \text{ harmonic component}} \tag{6}$$

where 3rd, 5th, and 7th respectively represent the third, fifth, and seventh leakage current harmonics components. In the case of the present study, odd harmonics until the 7th component were used to analyse the pollution severity on the surface of the insulator which is further clustered as below:

$$\begin{aligned} K_{(5+7)/3} &> \frac{THD}{n-1} && \text{Light} \\ \frac{THD}{n-1} &> K_{(5+7)/3} &> \frac{THD}{n+1} && \text{Medium} \\ K_{(5+7)/3} &< \frac{THD}{n+1} && \text{Heavy} \end{aligned} \tag{7}$$



where n is the number of odd harmonics until the 7th component.

III. EXPERIMENTAL SETUP

A. SPECIMEN PREPARATION

In the current research, two suspension types of insulators were adopted, namely the glass insulator and porcelain insulator. Table 2 tabulates the dimensions and parameters, as well as the profiles of both insulators. As can be observed, H is the insulator height, D refers to the insulator diameter, and L postulates the leakage distance. Meanwhile, the picture of a two-unit glass insulators string tested in contaminated conditions is depicted in Figure 2.

TABLE 2. Tested insulators parameters.

Profile	H(mm)	D(mm)	L(mm)	Type
	146	255	320	LXY1-70 (GLASS)
	146	255	305	XP-70 (Porcelain)

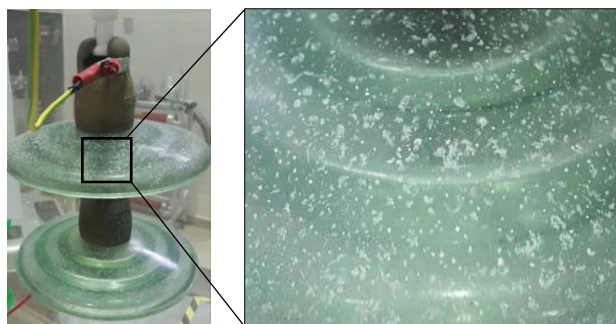


FIGURE 2. Contaminated glass insulator for laboratory testing.

TABLE 3. The test insulators strings.

Name of Insulator string	Disc number	Type	Operating voltage (kV)	THD%
SA	2	LXY1-70 (glass)	22	3.37
SB	3		33	4.69
SC	5		66	6.32
SD	2	PX-70 (Porcelain)	22	3.37
SE	3		33	4.69
SF	5		66	6.32

The set of insulators strings (SA, SB, SC, SD, SE, and SF) used for laboratory testing in the current work is tabulated in Table 3. Specifically, the applied voltages of 22-kV, 33-kV, and 66-kV AC were selected with THD of 4.37%, 5.69% and 7.32% respectively to simulate the operating voltage of distribution lines. Meanwhile, five different pollutions with different ratios of the NaCl solution were used as a soluble contaminant in representing clean, light, moderate, heavy, and very heavy polluted condition. In addition, the equivalent salt deposit density (ESDD) values were adjusted to model various levels of pollution as shown in Table 4.

As can be observed in Table 4, the ratio (R %) is defined as the amount of salt which is mixed in 1-litre water. In this case, the solid layer method was employed to apply the contaminants on the surface of the insulators [11], [31], [32]. Accordingly, the test specimens were sprayed with the prepared solutions and dried naturally at a temperature of 27 C ° for 24 hours before being suspended inside the chamber.

TABLE 4. ESDD and electrical conductivity for tested specimen.

R % Salt /water (g/1liter)	ESDD (mg/cm ²)	Measured electrical conductance (mS/cm)	Pollution severity
0.00	0.00	0.00	Clean
0.03	0.061	0.473	Light
0.05	0.122	1.326	Medium
0.1	0.208	2.287	Heavy
1.8	0.3	3.6897	V Heavy

Next, the values of ESDD were extracted by mixing different proportions of salt NaCl to 1-liter of distilled water (R%) (Table 4) considering that it will provide a direct effect on electrical conductivity σ of the polluted layer. Regarding this matter, approximately 40 (g/l) Kaolin powder can be used for non-soluble contaminant according to the IEC50607 standard [33].

Next, the insulators that were completely dried then suspended in an artificial test chamber made of polycarbonate sheet walls with the dimension of 50 cm x 50 cm x 75 cm. Specifically, a total of eight nozzles were placed around the internal wall of the chamber, fed from a compressed-air pipeline and a water pipeline.

Next, the polluted insulators were wetted with light, medium, and heavy fog conditions which are respectively represented by an approximate of 7 ± 0.5 g/s.cm³, 43.3 ± 1.5 g/s.cm³, and 83.8 ± 2.3 g/s.cm³ of flow rate. Apart from that, the chamber temperature was regulated between 26 C ° and 30 C °, while the relative humidity produced by the fog generator was maintained between 79% and 99%. The schematic diagram of the leakage current test used in the present study is shown in Figure 3.

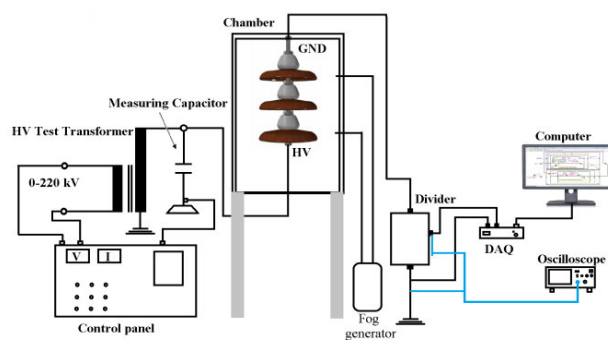


FIGURE 3. Schematic of the leakage current test circuit.

B. CONDUCTIVITY AND ESDD MEASUREMENT

The uniformly contaminated layer was carefully removed from the surface of the insulator to calculate the conductivity and equivalent salt deposit densities (ESDD), which was then

dissolved in 1-litre de-ionised water. Next, the conductivity of the solution was measured under room temperature using a conductivity meter HI8733. In this case, the conductivity σ and ESDD were calculated according to the IEC 60507 [33] as described in the following expressions:

$$ESDD = \frac{S_a \times V}{A} \quad (8)$$

$$S_a = 5.7 \times (\sigma_{20})^{1.03} \quad (9)$$

$$\sigma_{20} = \sigma_{\theta} \times [1 - b(\theta - 20)] \quad (10)$$

$$b = 0.9 \times 10^{-5}\theta^2 - 0.8 \times 10^{-3}\theta + 0.0353 \quad (11)$$

where σ_{20} defines the layer conductivity at 20°C, σ_{θ} is the volume conductivity at θ °C, θ postulates the temperature of the solution, and A refers to the area of insulator surface. As can be observed, S_a represents the salinity of the solution, V is the volume of the solution (cm³), and b is the factor depending on temperature θ which is found to be approximately equal to 0.02 at the test room temperature $\theta = 27$ °C [33].

The non-soluble deposit density (NSDD) was calculated based on the following expression [33]:

$$NSDD = \frac{(w_f - w_i) \times 10^3}{A} \quad (12)$$

where w_f is the weight of the filter paper containing pollutants, followed by w_i which describes the initial weight of the filter paper under dry conditions, and A represents the insulator surface area.

C. LEAKAGE CURRENT MEASUREMENT SETUP

In the current research, the diagnosis of contamination severity on the insulator surfaces was carried out in two stages, namely the measurement stage and investigation state. The measurement stage involves the process of transmitting measured data from tested insulator strings to the storage system during the test. Next, the investigation stage' was implemented using LABVIEW software with the main function of collecting and analysing data. Moreover, appropriate alarms will be generated when prospective hazardous pollution levels are detected. Specifically, the measurement stage was carried out in an artificial test chamber based on the following specifications: A 230 V/100 kV, 5 kVA, 50 Hz. Meanwhile, a single-phase transformer was used to provide single-phase AC voltage up to 66 kV to energise the tested samples, while the supply voltage was measured using a capacitive divider. Figures 3 and 4 demonstrate the experiment setup and pictorial view of the leakage current measurement system. As can be observed, the leakage current of polluted string insulators was measured using the voltage divider (1000:1) located between the top insulator cap and the ground electrode. The voltage divider was chosen based on the protection of monitoring and measuring equipment which can decrease the recorded data values within the allowable input voltage range of the DAQ card NI6024E (± 10 V) [34]. The results of the experiment were recorded using Data Acquisition

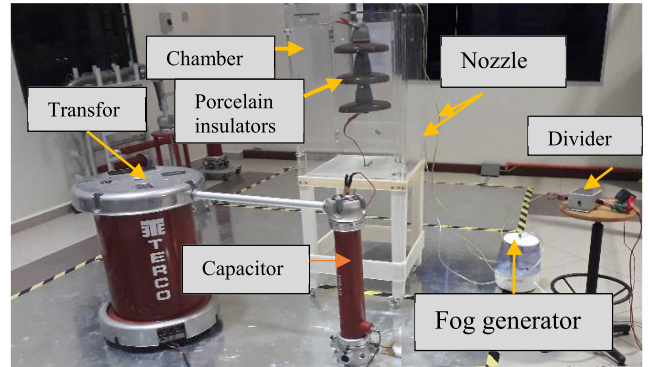


FIGURE 4. Laboratory setup.

System (DAQ) that is able to directly convert the measured voltage to leakage current.

Next, the measured leakage current was saved to the PC in CSV (MS-excel) file format. To the best of the author's knowledge, the leakage current test had to be repeated at least four times for each case; hence, the mean values of all recorded leakage currents were calculated as the final result.

The operating voltage for each group was energised after the wetting process of the contamination layer was completed. As mentioned above, the elaborated monitoring system is intended to measure the leakage current (LC) on the polluted insulators. The measured data will then be transferred to a collecting system where the data can be analysed to determine the pollution conditions of the insulators. Regarding this matter, it should be noted that the collecting system consists of two units, namely hardware and software. The software unit is utilized to take measurement from the DAQ card NI6024E, save the data, and then display it on a graphical interface. Apart from that, the software unit is also used to detect and manage alarms by generating warning messages. In the present study, software LabVIEW was employed for the implementation of the software interface of the supervision system. Specifically, the launching of the software was carried out by projecting a dialogue box on the display. The front panel allows the user to record the current session online, load an old session, or display the alarm history. Moreover, the interface of a current session shows the evolution time of LC, applied voltage, and spectrum analysis. Figure 5 presents the real-time leakage current and voltage signal waveform in the time and frequency domain. The graphical interface allows the monitoring and recording of data to:

- Display current and voltage waveform.
- Perform FFT analysis and display the values of harmonics as well as THD.
- Save the measured data to CSV (MS-excel) files for post-processing.

Figure 6 illustrates the diagram of the LabVIEW block which is the source code of the VI- the built-in language of graphical programming of LabVIEW. In addition, it should

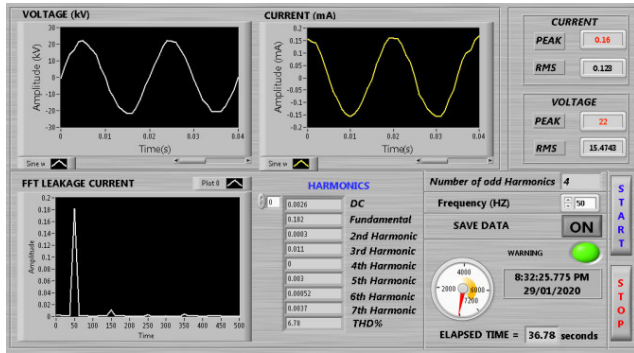


FIGURE 5. LabVIEW user interface panel.

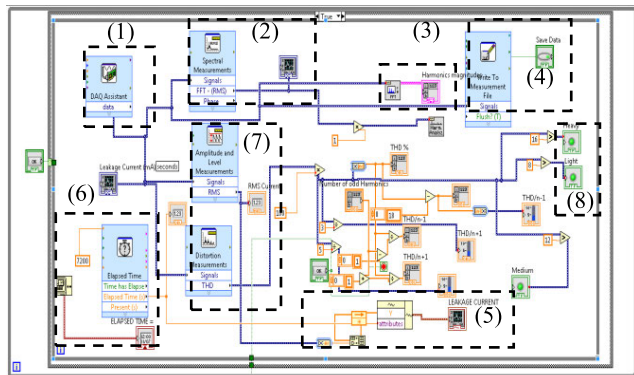


FIGURE 6. LabVIEW block diagram: (1) DAQ Block, (2) FFT transform waveform, (3) Show harmonics values, (4) Save data (5) Leakage current history, (6) Timer (7) Current and voltage waveform and (8) Start/stop.

be noted that the block diagram is the actual executable program consisting of built-in functions, constants, sub-VIs, and control structures for program execution. The LABVIEW program runs in conjunction with the test run for the purpose of capturing and storing data.

In this case, the alarms will be generated during the leakage current measurement, which indicates a dangerous situation. Meanwhile, the analysed saved data and alarm generating history can be read from the LabVIEW interface. More importantly, the odd harmonics, total harmonic distortion, and phase shift angle of the current waveforms have been determined as the main part of the diagnostic process. Regarding this matter, voltage distortions were also taken into account considering its sensitivity towards the changes in the level of pollution of insulator surface [35].

The total harmonic distortion was employed in the current research as a judgment on the degree of intensity of pollution. Apart from that, it was also aimed at studying the distorted LC signals resulted from the presence of discharges. In this case, it should be noted that the leakage current signals from the test sample are analogues in reality. In particular, these signals are subjected to digitising before arriving at PC using DAQ. Meanwhile, the signals were acquired by DAQ through a process known as sampling, followed by the digitising of the analogue samples. A sampled signal can be given as

follows [36]:

$$x_s(t) = g(t)x(t) \tag{13}$$

$$= \left(\sum_{n=-\infty}^{\infty} C_n e^{jn2\pi f_s t} \right) x(t) \tag{14}$$

$$= \sum_{n=-\infty}^{\infty} C_n x(t) e^{jn2\pi f_s t} \tag{15}$$

where $x(t)$ represents the periodic waveform at $t = n^*T$, T postulates the single sample period, C_n is the Fourier coefficient at T , and $g(t)$ describes the sampling function at $f_s = 1/T$. Meanwhile, the equation in the frequency domain is written as below:

$$X(f) = \int_{-\infty}^{\infty} x(t) e^{-j2\pi f t} dt \tag{16}$$

where f represents the frequency. In this case, the numerical integration was performed to calculate the Fourier transform to obtain the discrete Fourier transform (DFT) using the following expression:

$$X_k = \sum_{n=0}^{N-1} x_n e^{-j2\pi kn/N} \quad k = 1, 2 \dots N \tag{17}$$

where n represents the sample number.

IV. EXPERIMENTAL RESULTS AND DISCUSSION

A. VALIDATION OF LABVIEW SOFTWARE

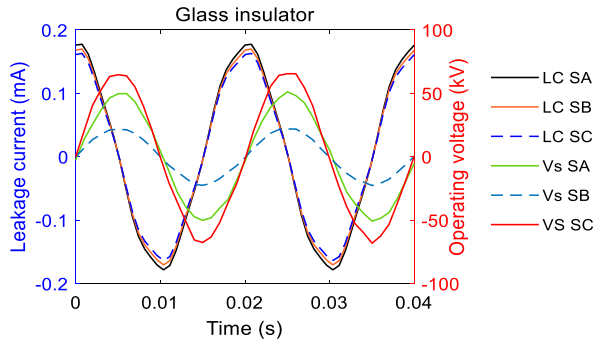
The results of the validation of LabVIEW software was carried out by comparing the achieved LabVIEW outcomes with those given by the oscilloscope connected in parallel. Table 5 presents the measurement of leakage current under several factors which are the light pollution level of 0.06 mg/cm² ESDD, fog rate of 7 ± 0.5 g/s.cm³, and operating voltage of 11kV.

TABLE 5. LabVIEW and oscilloscope results comparison.

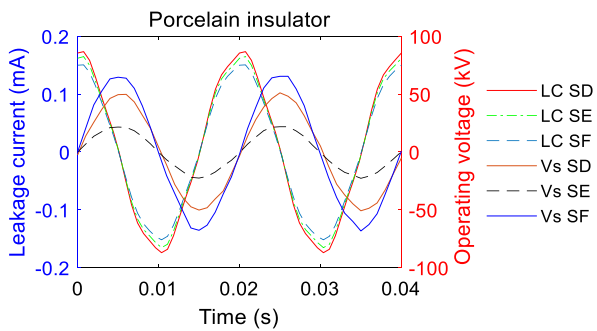
Leakage current characteristics	Results by LabVIEW	Results by oscilloscope	Error %
LC peak	0.814	0.187	0.002121
1st	0.796	0.799	0.001212
3rd	0.163	0.164	0.000707
5th	0.329	0.327	0.001414
7th	0.145	0.146	0.000707

B. LEAKAGE CURRENT COMPONENT OF CLEAN INSULATORS UNDER DRY CONDITION

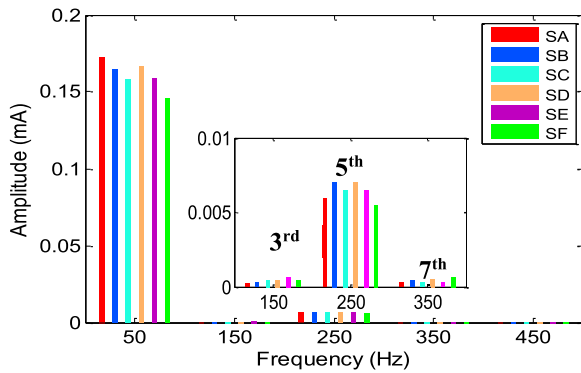
Figure 7 illustrates the time leakage current waveform and its FFT for the insulators string in clean condition for dry and different levels rate of fog. In this experiment, the operating voltage was energised for each string.



(a) Glass insulator



(b) Porcelain insulator



(c) FFT Odd harmonics of all the insulators strings.

FIGURE 7. Leakage current components of clean-dry insulators strings under operating voltage.

As can be observed, the LC values are very small in magnitude and predominantly capacitive with approximately 90° phase shift on a clean surface as shown in Table 6.

Nevertheless, no traces of flashover could be observed in this condition test. The harmonics and phase angle of leakage current are useful in understanding the behavior of the equivalent circuit of the insulator. In addition, it is important to mention that the indices of diagnostic were determined using odd harmonics, THD, and phase angle. In clean-dry case, the 3rd harmonic component always appears to be less than the 5th harmonic component as shown in Figure 7(c). Meanwhile, the phase shift angle was determined by calculating the difference between the angle of LC in normal

TABLE 6. Leakage current components in mA of clean insulators under dry condition and operating voltage for each string.

LC components	String insulators types - Operating voltage					
	SA	SB	SC	SD	SE	SF
	22 kV	33 kV	66 kV	22 kV	33 kV	66 kV
1st	0.176	0.168	0.161	0.171	0.162	0.15
3rd	0.0002	0.0003	0.0002	0.0004	0.0003	0.0002
5th	0.006	0.005	0.007	0.004	0.006	0.005
7th	0.003	0.001	0.001	0.0008	0.0006	0.003
THD	5.29%	4.44%	5.32%	4.57%	4.41%	4.52%
θ	≈ 90					

condition (using 90° as reference) and angle LC in the other conditions using FFT analysis of two cycles of the leakage current signal. The results for the insulator strings (SA, SB, SC, SD, SE, and SF) in clean and dry cases show that the peak values of leakage current are 0.176 mA, 0.168 mA, 0.161 mA, 0.171 mA, 0.162, and 0.150 mA, respectively.

C. LEAKAGE CURRENT COMPONENT OF CLEAN INSULATORS UNDER WET CONDITION

In the case of the present study, the clean insulators strings were tested under different levels of fog flow rate and operating voltage. The results of LC measured under three levels of wetness for insulator string A (SA) are illustrated in Figure 8. As can be observed, the result shows the insignificant influence of fog flow rate in leakage current amplitude on the clean insulators. However, a slight increase is notable in the LC value due to the increase in wetness rate when the samples were tested in clean condition. A possible explanation for this may be described by the presence of more water droplets that raises the conductance along the insulator surface. Consequently, this produced an easier path for flow current in the form of the positively and negatively charged ions that move from one electrode to another. Apart from that, the increase in the leakage current is clearly shown to be accompanied by an increase in phase shift angle δ due to the enhanced resistive current without a change in the capacitive current. For instance, the leakage current values of insulators string A (SA) are 0.176 mA, 0.226 mA, 0.284 mA, and 0.345 mA when the flow rate of fog are 0.00 g/s.cm³, 7 ± 0.5 g/s.cm³, 43.3 ± 1.5g/s.cm³, and 83.8 ± 2.3 g/s.cm³, respectively.

D. LEAKAGE CURRENT COMPONENT OF POLLUTED INSULATORS UNDER DRY CONDITION

In this section, LC measurement was carried out for the varying levels of pollution of insulators strings under dry condition. Figure 9 illustrates the leakage current waveform

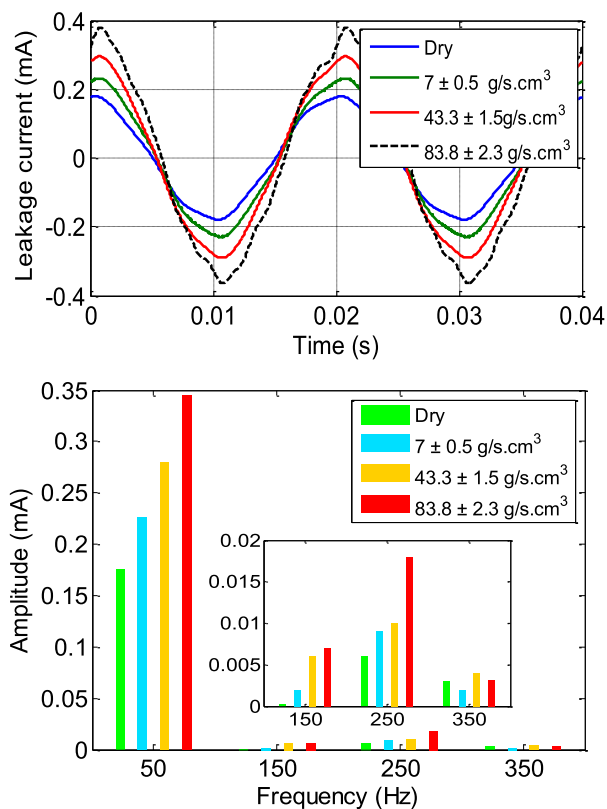


FIGURE 8. Leakage current waveform and its FFT for clean-wet insulator string A (SA) under different fog flow rates.

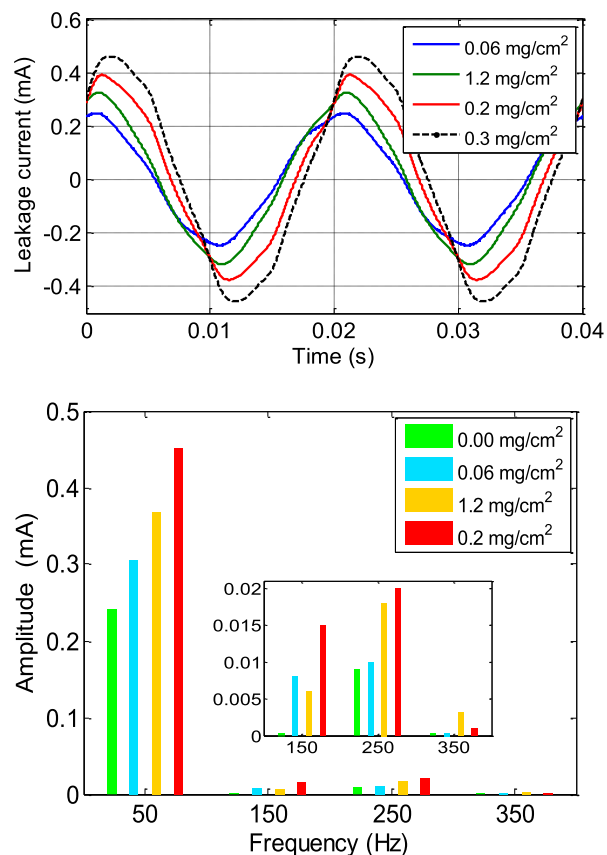


FIGURE 9. Leakage current waveform and its FFT for dry-pollution of insulator string A (SA) under different contamination levels.

and the frequency spectrum of the insulators string A (SA) for the considered ESDD (0.06, 0.14, 0.22 and 0.3 mg / cm²) with 0.15 mg/cm² NSDD under the operating applied voltage which occurred in a uniform pollution condition. According to Figure 9, no significant change in leakage current value can be observed for the varying levels of pollution (ESDD) under dry condition. As can be observed, the increase in the dry contamination severity on the surface insulator has caused the odd harmonics of leakage current to amplify itself. On the other hand, the sinusoidal waveform becomes less deformed with the decrease of the capacitive character of the pollution layer. Apart from that, it also decreases the insulator surface resistance [37]. More importantly, it should be noted that the increase in LC is accompanied by an increase in THD coefficient as well as the decrease in the LC phase shift resulted by the increased contamination severity for dry insulator string. For example, this can be observed in string insulator SA shown in Figure 10. The standard deviation obtained is between 0.12% and 0.24 %.

E. LEAKAGE CURRENT COMPONENT OF POLLUTED INSULATORS UNDER WET CONDITION

The result of the test showed no traces of flashover in normal condition. Moreover, it can be observed that the value of the 1st harmonic component of leakage current increases considerably with the increase in the wetting rate. Meanwhile, the 3rd harmonic of the leakage current appears to be less than the

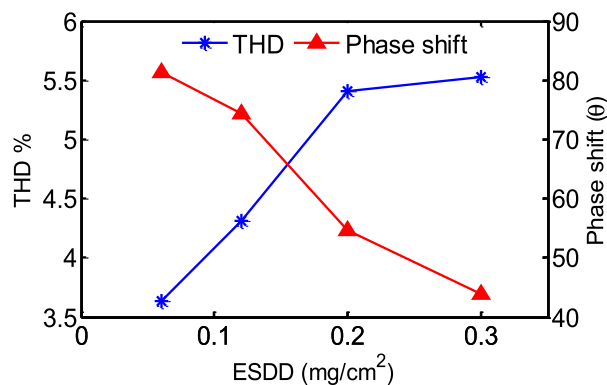


FIGURE 10. THD and LC phase shift against pollution level.

5th harmonic in the polluted insulators without the presence of fog. On the other hand, a significant change in odd harmonics (3rd, 5th, and 7th) can be detected when fog is applied and the wetting rate on the insulator surface is increased. Moreover, the 3rd harmonic started to escalate until it exceeds the 5th harmonic, while the value of the 7th harmonics increases and become approximately equal to the amount of 3rd harmonic. Regarding this matter, it is important to note that the changes in harmonics magnitude were resulted by the decrease in the pollution layer resistance due to the moisture absorption of

the fog. The increase in leakage current components for the 3rd, 5th, and 7th harmonics caused by the increase of the rate of wet and pollution level has led to the increase in the leakage current value I(t). Figure 11 and Figure 12 show the influence of the increase of wetting rate and contamination level on the leakage current components and THD of insulators string A (SA) under a standard applied voltage.

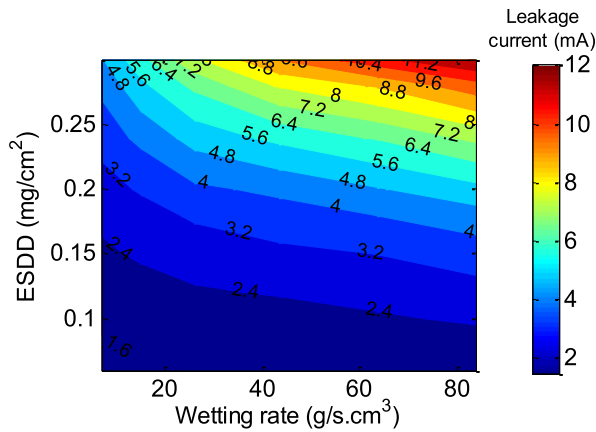


FIGURE 11. Leakage current with vary of ESDD and wetting rate for insulator string A (SA).

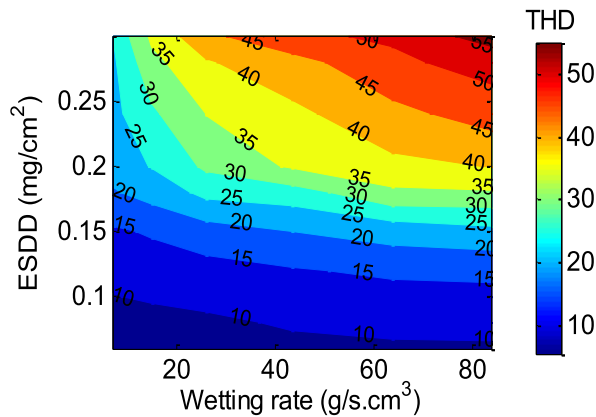


FIGURE 12. THD with vary of ESDD and wetting rate for insulator string A (SA).

Meanwhile, Table 7 provides the overall results obtained from the experimental tests for the leakage current components which include the magnitude, harmonics, THD, and phase shift for the tested insulators strings (SA, SB, SC, SD, SE, and SF) under different levels of contamination, namely light, medium, and heavy with the presence of different input rate of fog. The results of the LC measurements reported in Table 7 show that the leakage current in the condition of wet insulator increases remarkably compared to the clean state. Accordingly, this seems to suggest that the growth in wetting rate has a considerable influence on the growth of the odd harmonic of the leakage current as well as the behavior variations of the insulator. Hence, it can be expressed that the insulators are in a normal working state when the value of the 5th harmonic is higher than the 3rd. The increased

value of the leakage current harmonics components caused by the increased pollution further indicate the influence of wet-contamination on the behavior of electric of insulators.

On another note, the possibility of flashover occurrence is high when the wetting rate is high under pollution condition. Regarding this matter, it was found that the growth rate of 3rd harmonic prevailed over the 5th harmonic even though both the 3rd and 5th harmonics increased simultaneously. In addition, the insulator conditions became the most dangerous as the 3rd harmonic became higher than 5th, while the percentage of the flashover occurrence increased due to the increase in the electrical conductivity of the pollution layer.

The electrical conductivity in the surface of insulator increases with an increase in the amount of the dissolved salt and wetting rate of pollution layer, which increases the leakage current. On another note, the leakage current harmonic distortion (THD) increased in the high wetting rate level as a result of complete wetness and flow of liquid drops on the surface. Hence, this led to increased electrical conductivity on the insulator surface. Regarding this matter, it should be noted that the leakage current parameters including the total harmonics distortion and phase shift angle can be considered as an appropriate criterion in determining the pollution level. The total harmonics distortion showed a comparable tendency with LC magnitude of insulators, while the phase shift of LC was subjected to a significant drop due to the increased severity of contamination under wet condition. For example, the corresponding leakage current was 1.45 mA, 1.94 mA, 2.86 mA, and 4.72 mA for insulator string Type A (SA) under wetting rate of 7 ± 0.5 g/s.cm³ when the ESDD was 0.06, 0.12, 0.2, and 0.3 mg/cm², respectively. In addition, the leakage current under light wetness increased by 33.8%, 97.24%, and 225.5% when the ESDD was increased from 0.06 to 0.12, 0.2, and 0.3 mg/cm², respectively. Meanwhile, the percentage of leakage current under medium wetness was increased to 50.88%, 141.42%, and 466.3%, while the leakage current under high wetness condition rose by 50.52%, 177.6%, and 529.68%, respectively with the same increase in ESDD.

Figure 13 shows the relationship between the contamination level and wetting rate with the peak leakage current. Overall, the leakage current is expected to increase with the increase in the severity of contamination (ESDD) and wetting rate. The insulator that continues under operating voltage in light pollution condition remains to be properly functioning in all wet levels without any occurrence of flashover among the insulator strings. On another note, wetness is the most critical condition for the polluted insulator (especially in medium and heavy contamination severity) considering that a sudden increase in the surface conductivity of the insulator is triggered by the moistening of certain components of the pollution layer as well as the dissolving of soluble salts. Accordingly, this event ultimately contributes to the partial discharge on the insulator owing to the leakage flow and formatting of the dry bands. In the present study, some partial discharges and flashover process occurred at moderate and high fog rate under ESDD of 0.12, 0.2, and 0.3 mg/cm²

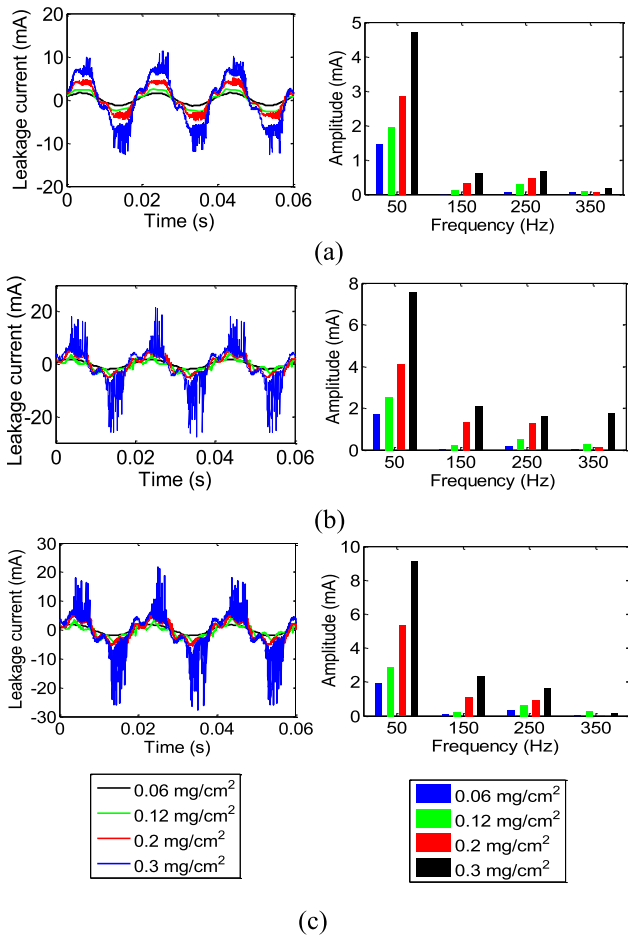


FIGURE 13. Time and frequency domains of leakage current for polluted insulators string A (SA) under (a) $7 \pm 0.5 \text{ g/s.cm}^3$, (b) $43.3 \pm 1.5\text{g/s.cm}^3$, (c) $83.8 \pm 2.3 \text{ g/s.cm}^3$.

(medium and heavy contamination levels) for all types of samples strings, which resulted in the appearance of pulses in the signal. Therefore, it is important to mention that the F sign shown in Table 7 indicates that the flashover occurred at a voltage less than the operating voltage on the insulator string.

V. DISCUSSION IN THE FUNCTION RANGE OF THE INDICES $K_{(5+7)/3}$

A. $K_{(5+7)/3}$ INDICATOR AND ITS OPERATING

Figures 14 to 16 show the simplified process of identifying and validating the proposed new technique concerning the odd and total harmonic as well as the distortion of the leakage current of SA, SC, and SF insulator strings which are used as a tool in the estimation of the contamination level. As previously mentioned, the variations of 3rd, 5th, and 7th harmonic components were adopted to evaluate the contamination severity of insulators under service condition.

Meanwhile, the THD to the number of odd harmonics ± 1 ($n \pm 1$) plays an important role in diagnosing the intensity of the pollution which is specifically used as limits.

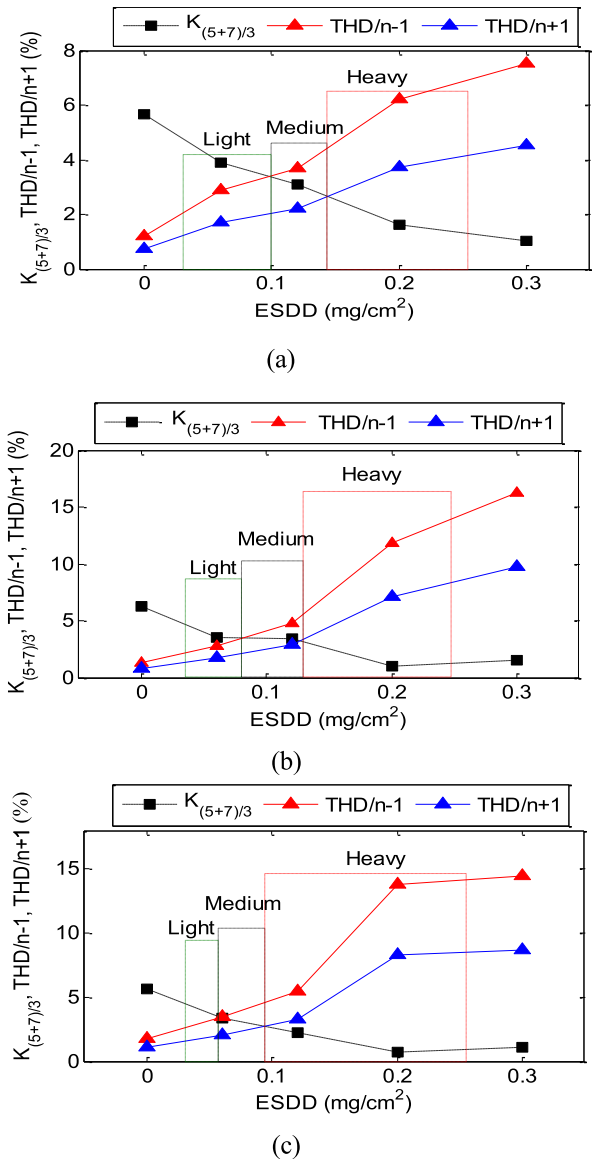


FIGURE 14. $K_{(5+7)/3}$, THD/n-1 and THD/n+1 for insulator string A (SA) at: (a) $7 \pm 0.5 \text{ g/s.cm}^3$, (b) $43.3 \pm 1.5\text{g/s.cm}^3$, (c) $83.8 \pm 2.3 \text{ g/s.cm}^3$.

The increase of total harmonic distortion and 3rd harmonic component, especially of LC was the result of surface pollution and several other factors such as humidity and temperature. Figures 14 to 16 present the new index $K_{(5+7)/3}$ and (THD/ $n \pm 1$) versus different levels of Equivalent Salt Deposit Density (ESDD) for the tested insulator in both single and string cases. In clean condition, $K_{(5+7)/3}$ index is shown to be greater than 5% for all tests when the 3rd harmonic is almost non-existent. Accordingly, it should be noted that this value is larger than THD/ $n+1$ and THD/ $n-1$ values with no occurrence of flashover. Hence, it can be noted that the insulators are in their clean condition when $K_{(5+7)/3}$ is greater than 4%. In the case of light pollution condition, the $K_{(5+7)/3}$ value appears to be more than THD/ $n+1$ and THD/ $n-1$ but not exceeding 4% except in some cases with light wetting

TABLE 7. Leakage current components in mA for different pollution levels and wetness rates under operating voltage for each string.

		String insulators types											
		SA 22kV	SB 33 kV	SC 66 kV	SD 22 kV	SE 33 kV	SF 66 kV	SA 22kV	SB 33 kV	SC 66 kV	SD 22 kV	SE 33 kV	SF 66 kV
Wetting rate g/s.cm ³	ESDD	0.06 mg/cm ²						0.12 mg/cm ²					
	LC Components												
7±0.5	1 st Component	1.45	1.23	1.32	1.37	1.29	1.22	1.94	2.214	2.22	1.87	1.71	1.68
	3 rd Component	0.02	0.013	0.06	0.05	0.07	0.09	0.13	0.15	0.2	0.11	0.13	1.12
	5 th Component	0.05	0.03	0.17	0.14	0.18	0.16	0.31	0.18	0.27	0.27	0.26	0.26
	7 th Component	0.05	0.04	0.15	0.13	0.14	0.19	0.07	0.05	0.04	0.06	0.05	0.08
	THD %	5.48	8.41	8.52	7.25	9.52	8.59	11.8	12.04	11.39	10.85	10.52	11.09
43.3±1.5	1 st Component	1.69	1.47	1.41	1.59	1.47	1.46	2.55	2.26	2.27	2.29	2.27	2.16
	3 rd Component	0.04	0.07	0.1	0.09	0.11	0.1	0.23	0.25	0.26	0.27	0.24	0.25
	5 th Component	0.15	0.11	0.23	0.16	0.15	0.2	0.49	0.43	0.49	0.41	0.41	0.48
	7 th Component	0.03	0.09	0.2	0.15	0.12	0.18	0.29	0.25	0.21	0.16	0.15	0.14
	THD %	8.44	9.76	9.48	8.21	8.81	9.06	14.5	13.75	14.63	14.21	13.81	14.06
83.8±2.3	1 st Component	1.92	1.84	1.76	1.86	1.82	1.71	2.89	2.73	2.55	2.66	2.42	2.41
	3 rd Component	0.1	0.16	0.12	0.09	0.11	0.12	0.25	0.28	0.27	0.18	0.17	0.25
	5 th Component	0.32	0.14	0.24	0.21	0.16	0.23	0.62	0.56	0.48	0.31	0.42	0.55
	7 th Component	0.08	0.15	0.22	0.15	0.16	0.17	0.27	0.23	0.22	0.15	0.21	0.23
	THD %	9.05	11.06	10.21	9.82%	10.47	10.31	15.22	15.56	14.43	15.82	16.4	16.23
	θ°	31.3	38.7	34.74	28.2	29.5	30.4	20.6	18.7	20.1	18.2	19.5	20.4
Wetting rate g/s.cm ³	ESDD	0.2 mg/cm ²						0.3 mg/cm ²					
	LC Components												
7±0.5	1 st Component	2.86	3.214	2.62	2.7	2.95	2.41	4.72	4.214	4.22	3.7	3.59	4.211
	3 rd Component	0.33	0.31	0.35	0.29	0.23	0.23	0.62	0.63	0.55	0.52	0.74	0.63
	5 th Component	0.47	0.37	0.25	0.22	0.29	0.27	0.67	0.57	0.46	0.58	0.51	0.47
	7 th Component	0.06	0.1	0.07	0.11	0.14	0.1	0.18	0.12	0.13	0.11	0.11	0.19
	THD %	21.94	23.46	19.9	23.61	16.52	18.59	25.17	23.46	23.39	21.61	21.52	22.59
43.3±1.5	1 st Component	4.08	4.26	4.05	4.29	4.11	3.96	9.57	8.26	9.27	F	8.87	9.03
	3 rd Component	1.34	0.9	1.1	1.07	0.95	1.15	2.12	2.05	1.96	F	2.14	2.25
	5 th Component	1.25	0.7	0.9	0.87	0.75	0.64	1.59	1.43	1.29	F	1.41	1.28
	7 th Component	0.14	0.17	0.14	0.26	0.25	0.34	1.73	1.15	1.24	F	1.15	1.34
	THD %	35.63	33.75	34.63	33.21	31.81	32.06	48.81	49.75	46.63	F	45.24	44.06
83.8±2.3	1 st Component	5.33	5.73	0.35	0.36	0.32	0.31	12.09	F	12.35	F	F	11.31
	3 rd Component	1.13	1.08	1.17	1.28	1.07	1.55	3.38	F	2.97	F	F	2.75
	5 th Component	0.97	1.16	1.08	0.821	1.02	1.015	2.63	F	2.18	F	F	1.95
	7 th Component	0.04	0.1	0.08	0.05	0.09	0.1	1.14	F	1.42	F	F	1.13
	THD %	40.15	35.56	37.43	35.82	39.47	41.31	57.23	F	45.43	F	F	43.31
	θ°	12.2	7.7	6.1	8.2	9.5	8.4	4.3	F	2.1	F	F	1.4

rates. Moreover, there is no possibility of flashover occurring in this range due to the continuously high surface resistance in these conditions. However, flashover may occur at 0.06 mg/cm² with heavy wetting rate due to the light conductive layer with high electrical stress. In light pollution condition, the 3rd harmonic seemed to increase but not exceeding the 5th harmonics component. In the medium contamination severity condition, the $K_{(5+7)/3}$ index was reduced to a value lower than THD/n-1 but remained above THD/n+1. Overall, the $K_{(5+7)/3}$ value remained between THD/n-1 and

THD/n+1 in this case. More importantly, this confirms that the conductance value of the insulator surface experienced a higher increase in moderate pollution level with salt deposit density compared to the light pollution level.

The increase in the contamination level increases led to the increase of the 3rd harmonic but not exceeding the 5th and 7th harmonic values. Hence, the value of the proposed index $K_{(5+7)/3}$ dramatically decreased compared to its value in the condition of light pollution. Meanwhile, the decrease in the index value which is lower than THD /n+1 in some

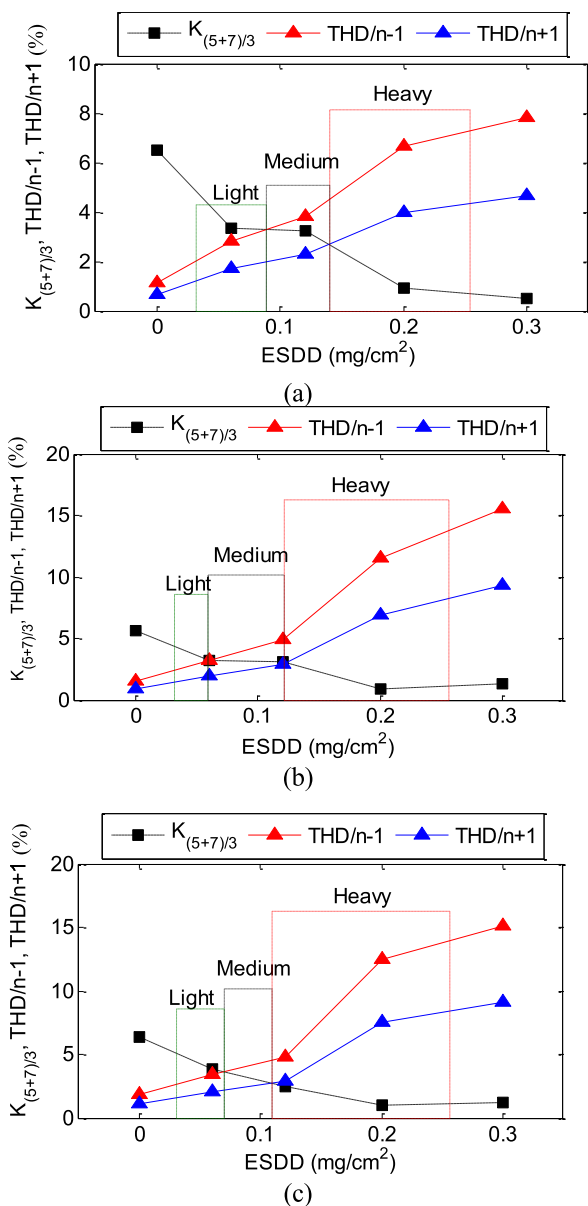


FIGURE 15. $K_{(5+7)/3}$, THD/n-1 and THD/n+1 for insulator string C (SC) at: (a) 7 ± 0.5 g/s.cm³, (b) 43.3 ± 1.5 g/s.cm³, (c) 83.8 ± 2.3 g/s.cm³.

moderate pollutions and wetting rate of 83.8 g/s.cm³ indicates a higher flashover occurrence probability. More importantly, the increase in contamination severity level to a high value will increase the electric conductance, which causes the $K_{(5+7)/3}$ value to continue to subside to a value less than THD/n-1 and THD/n+1 that may be as low as 2%. Accordingly, this seems to suggest that the $K_{(5+7)/3}$ will be less than THD/n-1 and THD/n+1 in the heavy contamination level condition as well as several medium levels with a heavy wetting rate similar to the results presented in Figures 14 to 16 (c). The 3rd harmonic in this pollution level demonstrates an increase which is larger than the 5th and 7th harmonics due to the increase in electric conductance of insulator surface. Under operating voltage, it can be observed that the total

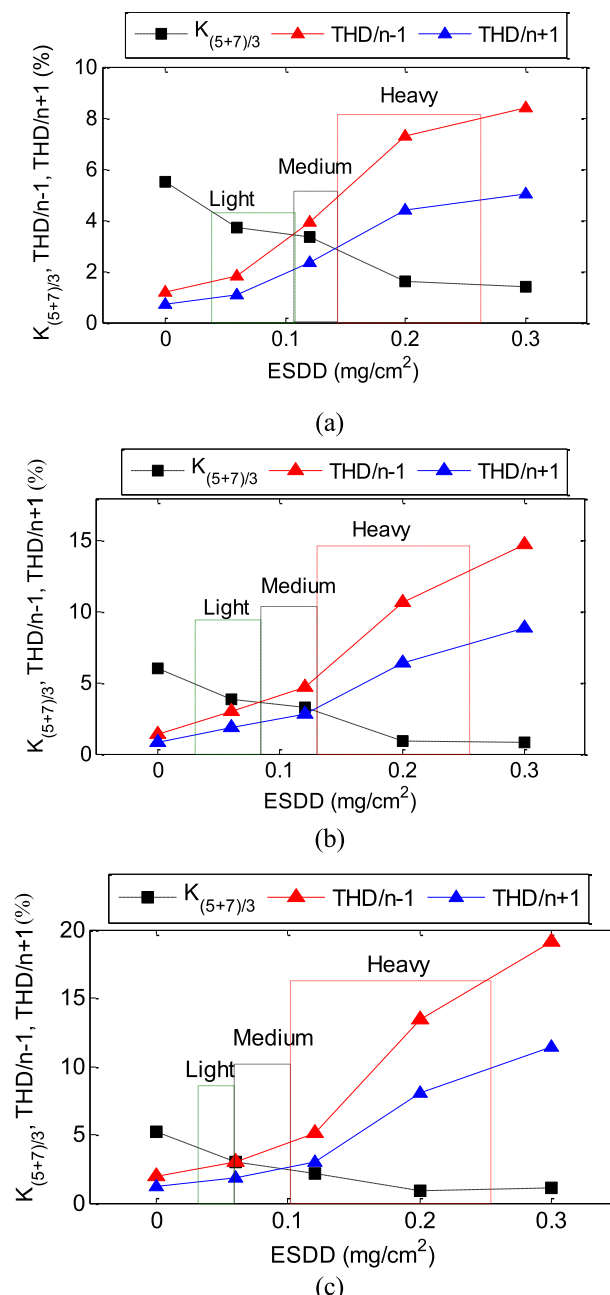


FIGURE 16. $K_{(5+7)/3}$, THD/n-1 and THD/n+1 for insulator string F (SF) at: (a) 7 ± 0.5 g/s.cm³, (b) 43.3 ± 1.5 g/s.cm³, (c) 83.8 ± 2.3 g/s.cm³.

harmonic deformation THD increases with the increase in pollution intensity and the wetting rate of the pollution layer. Table 7 presents the measured amounts whereby the increase in the contamination level in the low wetting rate has resulted in an approximately equal increase of THD percentage at all pollution levels. Meanwhile, the THD in the high wetting rate is shown to have a significant increase at the heavy pollution level as presented in Figures 14 to 16. However, the THD may give the excellent indicating for insulator condition, but in some clean state appears High. So, the THD alone not enough to diagnostic state of insulators. Generally, the 3rd harmonic

TABLE 8. The strings insulators situation according to $K_{(5+7)/3}$ and THD limited.

$K_{(5+7)/3}\%$	Insulator conditions						Pollution Level based to THD boundaries
	Normal		Medium		Critical		
>3	SC	Yes	SC	-	SC	-	Clean and Light and ($K_{(5+7)/3} > THD/n-1$)
	SF	Yes	SF	-	SF	-	
(3-2)	SC	Yes	SC	Yes	SC	-	Medium and ($THD/n-1 > K_{(5+7)/3} > THD/n+1$)
	SF	-	SF	Yes	SF	-	
(2-1.7)	SC	-	SC	Yes	SC	-	Heavy and ($K_{(5+7)/3} < THD/n+1$)
	SF	-	SF	-	SF	Yes	
< 1.7	SC	-	SC	-	SC	Yes	Heavy and ($K_{(5+7)/3} < THD/n+1$)
	SF	-	SF	-	SF	Yes	

in the critical condition insulators under operating voltage before the occurrence of the flashover tends to be larger than 5th harmonic, while the proposed indicator is commonly lower than 2%.

B. DETERMATION OF INSULATORS CONDITIONS

In Table 8, the glass group (SC) and porcelain group (SF) insulators conditions are listed according to the $K_{(5+7)/3}$ index range as well as the $THD/n-1$ and $THD/n+1$ boundaries which are represented as normal, moderate deterioration, and critical described below:

- Normal: no electric discharge.
- Moderate deterioration: some visible point discharge with continuous sound and linear weak local arcs.
- Critical: intermittent, strong local arcs (before flashover).

The experimental tests were conducted on 96 cases (6 cases clean-dry + 18 clean-wet + 72 cases wet pollution). In particular, the conditions for 46 cases were critical, followed by $K_{(5+7)/3} < 2\%$ for porcelain, and $K_{(5+7)/3} < 1.7$ for glass insulators. Hence, the two ranges of the $K_{(5+7)/3}$ index can be considered as a range of critical conditions where the probability of flashover occurrence is high. Regarding this matter, it should be noted that all these critical cases tend to occur when $K_{(5+7)/3}$ is lower than $THD/n+1$ (heavy pollution) for low and medium wetness, while the critical condition is $K_{(5+7)/3} < THD/n-1$ and $THD/n+1$ (medium and heavy pollutions) under high wetness.

According to the results of the test, all of the six tests conducted for clean and dry insulator were diagnosed using the proposed technique $K_{(5+7)/3}$ without any error. Meanwhile, 17 out of 18 tests were recorded as a correct diagnostic by $K_{(5+7)/3}$ indicator for clean and wet insulators, which is equivalent to 94.4% of the tests. The diagnosis of the $K_{(5+7)/3}$ indicator for a total of 67 out of 72 tests was true under the wet-pollution condition for insulators. More importantly, this is equivalent to 93% of the tests.

In total, the indicator correctly recorded 90 out of 96 tests which are represented by the indicator $K_{(5+7)/3}$ efficiency of 93.7% for all the tests.

VI. CONCLUSION

The current research successfully proposed and verified a new technique based on harmonics component of leakage current which is referred to as $K_{(5+7)/3}$ indicator, particularly regarding the improvement of monitoring and diagnosis of contamination severity for glass and porcelain insulators. In the case of the present study, the insulator strings under salt-fog pollution condition represented by three contamination levels, namely light, medium, and high were selected to determine a diagnostic criterion. Meanwhile, the experimental results of the tested insulators strings under different operation voltage (22kV, 33kV, and 66kV) were presented in this paper, followed by the conclusions drawn as follows:

1. The odd harmonics till the 7th component of leakage current can be utilized to establish a good correlation with the pollution severity level on the insulator surfaces.
2. The proposed index, $K_{(5+7)/3}$ can be effectively used as a tool to predict the pollution severity of an outdoor insulator. The insulator is considered under a normal and clean condition if $K_{(5+7)/3} > 3\%$. Next, pollution severity is classified as moderate if $2\% < K_{(5+7)/3} < 3\%$, while the pollution level is considered to be in heavy or extreme condition if $K_{(5+7)/3} < 2\%$.
3. The insulator is predicted to be in a critical condition when $K_{(5+7)/3} < 1.7\%$ whereby the probability of flashover occurrence is high.
4. The proposed technique can be a promising approach in the prediction of pollution severity on insulator. Apart from that, it can also be effectively implemented on any type of insulators with the respective boundary conditions in the attempt to predict the contamination level and flashover likelihood on outdoor insulators.

REFERENCES

- [1] A. Said, "Analysis of 500 kV OHTL polluted insulator string behavior during lightning strokes," *Int. J. Electr. Power Energy Syst.*, vol. 95, pp. 405–416, Feb. 2018.
- [2] J. Mahmoodi, M. Mirzaie, and A. A. Shayegani-Akmal, "Surface charge distribution analysis of polymeric insulator under AC and DC voltage based on numerical and experimental tests," *Int. J. Electr. Power Energy Syst.*, vol. 105, pp. 283–296, Feb. 2019.
- [3] M. Ramesh, L. Cui, and R. S. Gorur, "Impact of superficial and internal defects on electric field of composite insulators," *Int. J. Electr. Power Energy Syst.*, vol. 106, no. 6, pp. 327–334, Mar. 2019.
- [4] Z. Zhang, X. Liu, X. Jiang, J. Hu, and D. W. Gao, "Study on AC flashover performance for different types of porcelain and glass insulators with non-uniform pollution," *IEEE Trans. Power Del.*, vol. 28, no. 3, pp. 1691–1698, Jul. 2013.
- [5] J. Wardman, T. Wilson, S. Hardie, and P. Bodger, "Influence of volcanic ash contamination on the flashover voltage of HVAC outdoor suspension insulators," *IEEE Trans. Dielectr. Electr. Insul.*, vol. 21, no. 3, pp. 1189–1197, Jun. 2014.
- [6] Z. Shihua, J. Xingliang, Z. Zhijin, and H. Jianlin, "Flashover voltage prediction of polluted glass insulators based on the characteristics of leakage current," (in Chinese), *Power Syst. Technol.*, vol. 38, no. 2, pp. 440–447, Feb. 2014.
- [7] L. Ye, W. Zhou, S. Yang, L. Li, and J. Yu, "Effects of contaminations on voltage distribution along insulator string," *High Voltage App.*, vol. 15, no. 9, pp. 103–108, Sep. 2015.
- [8] N. Bashir and H. Ahmad, "Odd harmonics and third to fifth harmonic ratios of leakage currents as diagnostic tools to study the ageing of glass insulators," *IEEE Trans. Dielectr. Electr. Insul.*, vol. 17, no. 3, pp. 819–832, Jun. 2010.

- [9] T. Las, "Impact of corona on the long-term performance of nonceramic insulators," *IEEE Trans. Dielectr. Electr. Insul.*, vol. 11, no. 5, pp. 913–915, Oct. 2004.
- [10] L. Lan, G. Zhang, Y. Wang, X. Wen, W. Wang, and H. Pei, "The influence of natural contamination on pollution flashover voltage waveform of porcelain insulators in heavily polluted area," *IEEE Access*, vol. 7, pp. 121395–121406, 2019.
- [11] X. Zhang, J. Zhu, S. Bu, Q. Li, V. J. Terzija, and S. M. Rowland, "The development of low-current surface arcs under clean and salt-fog conditions in electricity distribution networks," *IEEE Access*, vol. 6, pp. 15835–15843, 2018.
- [12] N. Dhahbi-Megrache and A. Beroual, "Time–frequency analyses of leakage current waveforms of high voltage insulators in uniform and non-uniform polluted conditions," *IET Sci., Meas. Technol.*, vol. 9, no. 8, pp. 945–954, Nov. 2015.
- [13] A. H. El-Hag, S. H. Jayaram, and E. A. Cherney, "Fundamental and low frequency harmonic components of leakage current as a diagnostic tool to study aging of RTV and HTV silicone rubber in salt-fog," *IEEE Trans. Dielectr. Electr. Insul.*, vol. 10, no. 1, pp. 128–136, Feb. 2003.
- [14] H. H. Kordkheili, H. Abravesh, M. Tabasi, M. Dakhem, and M. M. Abravesh, "Determining the probability of flashover occurrence in composite insulators by using leakage current harmonic components," *IEEE Trans. Dielectr. Electr. Insul.*, vol. 17, no. 2, pp. 502–512, Apr. 2010.
- [15] C. N. Richards and J. D. Renowden, "Development of a remote insulator contamination monitoring system," *IEEE Trans. Power Del.*, vol. 12, no. 1, pp. 389–397, Jan. 1997.
- [16] E. Fontana, J. F. Martins-Filho, S. C. Oliveira, F. J. M. M. Cavalcanti, R. A. Lima, G. O. Cavalcanti, T. L. Prata, and R. B. Lima, "Sensor network for monitoring the state of pollution of high-voltage insulators via satellite," *IEEE Trans. Power Del.*, vol. 27, no. 2, pp. 953–962, Apr. 2012.
- [17] B. Moula, A. Mekhaldi, M. Tegar, and A. Haddad, "Characterization of discharges on non-uniformly polluted glass surfaces using a wavelet transform approach," *IEEE Trans. Dielectr. Electr. Insul.*, vol. 20, no. 4, pp. 1457–1466, Aug. 2013.
- [18] Y. Kemari, A. Mekhaldi, and M. Tegar, "Experimental investigation and signal processing techniques for degradation assessment of XLPE and PVC/B materials under thermal aging," *IEEE Trans. Dielectr. Electr. Insul.*, vol. 24, no. 4, pp. 2559–2569, 2017.
- [19] M. Douar, A. Mekhaldi, and M. Bouzidi, "Flashover process and frequency analysis of the leakage current on insulator model under non-uniform pollution conditions," *IEEE Trans. Dielectr. Electr. Insul.*, vol. 17, no. 4, pp. 1284–1297, Aug. 2010.
- [20] M. F. Palangar and M. Mirzaie, "Diagnosis of porcelain and glass insulators conditions using phase angle index based on experimental tests," *IEEE Trans. Dielectr. Electr. Insul.*, vol. 23, no. 3, pp. 1460–1466, Jun. 2016.
- [21] Z. Sahli, A. Mekhaldi, R. Boudissa, and S. Boudrahem, "Prediction parameters of dimensioning of insulators under non-uniform contaminated conditions by multiple regression analysis," *Electr. Power Syst. Res.*, vol. 81, no. 4, pp. 821–829, Apr. 2011.
- [22] H. Terrab and A. Bayadi, "Experimental study using design of experiment of pollution layer effect on insulator performance taking into account the presence of dry bands," *IEEE Trans. Dielectr. Electr. Insul.*, vol. 21, no. 6, pp. 2486–2495, Dec. 2014.
- [23] Y. Liu and B. Du, "Recurrent plot analysis of leakage current on flashover performance of rime-iced composite insulator," *IEEE Trans. Dielectr. Electr. Insul.*, vol. 17, no. 2, pp. 465–472, Apr. 2010.
- [24] J. Li, W. Sima, C. Sun, and S. Sebo, "Use of leakage currents of insulators to determine the stage characteristics of the flashover process and contamination level prediction," *IEEE Trans. Dielectr. Electr. Insul.*, vol. 17, no. 2, pp. 490–501, Apr. 2010.
- [25] B. Dong, X. Jiang, J. Hu, L. Shu, and C. Sun, "Effects of artificial polluting methods on AC flashover voltage of composite insulators," *IEEE Trans. Dielectr. Electr. Insul.*, vol. 19, no. 2, pp. 714–722, Apr. 2012.
- [26] Aulia, F. David, E. Waldy, and H. Hazmi, "The leakage current analysis on 20 kV suspension porcelain insulator contaminated by salt moisture and cement dust in padang area," in *Proc. IEEE 8th Int. Conf. Properties Appl. Dielectric Mater.*, Bali, Indonesia, Jun. 2006, pp. 384–387.
- [27] T. Suda, "Frequency characteristics of leakage current waveforms of a string of suspension insulators," *IEEE Trans. Power Del.*, vol. 20, no. 1, pp. 481–487, Jan. 2005.
- [28] A. H. El-Hag, "Leakage current characterization for estimating the conditions of non-ceramic insulators' surfaces," *Electr. Power Syst. Res.*, vol. 77, nos. 3–4, pp. 379–384, Mar. 2007.
- [29] H. K. E. Ahmed and Y. Kh, "Harmonics generation, propagation and purging techniques in non-linear loads," *Update Power Qual.*, vol. 47, pp. 777–780, Mar. 2013.
- [30] H. Ahmad, M. A. Salam, L. Y. Ying, and N. Bashir, "Harmonic components of leakage current as a diagnostic tool to study the aging of insulators," *J. Electrostatics*, vol. 66, nos. 3–4, pp. 156–164, Mar. 2008.
- [31] Z. Zhang, X. Qiao, Y. Xiang, and X. Jiang, "Comparison of surface pollution flashover characteristics of RTV (Room temperature Vulcanizing) coated insulators under different coating damage modes," *IEEE Access*, vol. 7, pp. 40904–40912, 2019.
- [32] A. Banik, S. Dalai, and B. Chatterjee, "Autocorrelation aided rough set based contamination level prediction of high voltage insulator at different environmental condition," *IEEE Trans. Dielectr. Electr. Insul.*, vol. 23, no. 5, pp. 2883–2891, Oct. 2016.
- [33] *Artificial Pollution Tests on High-Voltage Insulators to be Used on A.C. Systems*, document IEC 60507, International Electrotechnical Commission, Geneva, Switzerland, 2013.
- [34] *The Fundamentals of FFT-Based Signal Analysis and Measurement in LabVIEW and LabWindows/CVI*, LabVIEW, National Instrum., Austin, TX, USA, 2006.
- [35] R. Ghosh, B. Chatterjee, and S. Chakravorti, "A novel leakage current index for the field monitoring of overhead insulators under harmonic voltage," *IEEE Trans. Ind. Electron.*, vol. 65, no. 2, pp. 1568–1576, Feb. 2018.
- [36] N. Bashir, H. Ahmad, and M. A. B. Sidik, "An intelligent diagnostic system for condition monitoring of ageing glass insulators," *Int. Rev. Model. Simul.*, vol. 4, no. 5, pp. 2512–2518, 2011.
- [37] X. Zhang, A. Bruce, S. Rowland, V. Terzija, and S. Bu, "Modeling the development of low current arcs and arc resistance simulation," *IEEE Trans. Dielectr. Electr. Insul.*, vol. 25, no. 6, pp. 2049–2057, Dec. 2018.



ALI A. SALEM (Member, IEEE) was born in Sana'a, Yemen, in March 1985. He received the M.Eng. degree in electrical power engineering from University Tun Hussein Onn Malaysia (UTHM), from 2014 to 2016. He is currently pursuing the Ph.D. degree in high voltage with the Faculty of Electrical Engineering, UTHM. His research interest includes dynamic arc modeling of pollution flashover on high-voltage outdoor insulators.



R. ABD-RAHMAN was born in Kedah, Malaysia, in 1984. He received the M.Eng. degree in electrical and electronic engineering from Cardiff University, U.K., in 2008, and the Ph.D. from the High Voltage and Energy Systems, in 2012. After his graduation, he joined University Tun Hussein Onn Malaysia (UTHM) as an Academic Staff and a Research Fellow. He is currently a Lecturer with the University of Tun Hussein Onn Malaysia (UTHM), Batu Pahat, Malaysia.



SAMIR AHMED AL-GAILANI received the Ph.D. degree in optoelectronics from University Technology Malaysia (UTM), in 2014. He started his career as a Senior Lecturer at the Higher Technical Institute for applied B.Sc. degree Aden Yemen, in 1992. He has authored 20 ISI articles and has an H-Index of seven and total citations of 212, presented more than 90 articles in reputed refereed conferences. He also successfully supervised nine undergraduate students. During his Ph.D. degree, he received the award and since then has been given various responsibilities including a Teaching, Postdoctoral Fellow, a Supervising Laboratory Sessions, a Supervising Post-Graduate Students and Undergraduate Students, an Academic Advisor, the Head Of Laboratory, the Head of Research Group, the Chairman and a Member of Different Committees, and the Conducting Short Courses and Training.



M. S. KAMARUDIN (Member, IEEE) received the B.Eng. and M.Eng. degrees in electrical engineering (Power) from the University Technology Malaysia (UTM), in 2003 and 2005, respectively, and the Ph.D. in high voltage engineering from Cardiff University, U.K., in 2014. He is currently a Senior Lecturer with the Faculty of Electrical and Electronic Engineering, University Tun Hussein Onn Malaysia (UTHM). His research interests include gas discharges, high-voltage surge arresters, and dielectrics and electrical insulation systems. He is registered with the Board of Engineers Malaysia (BEM). He is also a Graduate Member of Institution of Engineers, Malaysia (IEM).



HUSSEIN AHMAD was born in 1953. He received the B.Sc. degree in electrical and electronic engineering, and the M.Sc. degree in electrical power engineering from the University of Strathclyde, Glasgow, in 1977 and 1981 respectively, and the Ph.D. degree in high voltage engineering from the UMIST, University of Manchester, in 1986. He was a Contract Professor with the University of Tun Hussein Onn Malaysia (UTHM), Batu Pahat, Malaysia, and the Research Center of Applied Electromagnetics, Faculty of Electrical and Electronic Engineering, UTHM. He is currently an Adjunct Professor at IVAT, UTM, for the period of 2018–2020.



ZAINAL SALAM (Member, IEEE) received the B.Sc. degree in electronics engineering from California State University, Chico, CA, USA, in 1985, the M.E.E. degree in electrical engineering from University Technology Malaysia (UTM), Kuala Lumpur, Malaysia, in 1989, and the Ph.D. degree in power electronics from the University of Birmingham, Birmingham, U.K., in 1997, respectively. He is currently a Professor in power electronics and renewable energy with the Centre of Electrical Energy Systems, Faculty of Electrical Engineering, UTM. He represents the country as an Expert for the International Energy Agency PV Power Systems Task 13 Working Group, which focuses on the reliability and performance of photovoltaic power systems. His main research interests include all areas of design, instrumentation, and control of power electronics and renewable energy systems. He was the Vice-Chair of the IEEE Power Electronics, Industrial Electronics, and Industry Application Joint Chapter, Malaysia Section, from 2011 to 2013, and in 2016. From 2011 to 2013, he was the Editor of the IEEE Transactions on Sustainable Energy.

• • •